

Minerva Access is the Institutional Repository of The University of Melbourne

Author/s:

Roberts, BR;Lim, NKH;McAllum, EJ;Donnelly, PS;Hare, DJ;Doble, PA;Turner, BJ;Price, KA;Lim, SC;Paterson, BM;Hickey, JL;Rhoads, TW;Williams, JR;Kanninen, KM;Hung, LW;Liddell, JR;Grubman, A;Monty, JF;Llanos, RM;Kramer, DR;Mercer, JFB;Bush, AI;Masters, CL;Duce, JA;Li, QX;Beckman, JS;Barnham, KJ;White, AR;Crouch, PJ

Title:

Oral treatment with Cull(atSm) increases mutant SOD1 in vivo but protects motor neurons and improves the phenotype of a transgenic mouse model of amyotrophic lateral sclerosis

Date:

2014-01-01

Citation:

Roberts, B. R., Lim, N. K. H., McAllum, E. J., Donnelly, P. S., Hare, D. J., Doble, P. A., Turner, B. J., Price, K. A., Lim, S. C., Paterson, B. M., Hickey, J. L., Rhoads, T. W., Williams, J. R., Kanninen, K. M., Hung, L. W., Liddell, J. R., Grubman, A., Monty, J. F., Llanos, R. M. ,... Crouch, P. J. (2014). Oral treatment with Cull(atSm) increases mutant SOD1 in vivo but protects motor neurons and improves the phenotype of a transgenic mouse model of amyotrophic lateral sclerosis. *Journal of Neuroscience*, 34 (23), pp.8021-8031. <https://doi.org/10.1523/JNEUROSCI.4196-13.2014>.

Persistent Link:

<https://hdl.handle.net/11343/51371>

Oral treatment with Cu^{II}(atsm) increases mutant SOD1 *in vivo* but protects motor neurons and improves the phenotype of a transgenic mouse model of amyotrophic lateral sclerosis

Abbreviated title: Cu^{II}(atsm) and mutant SOD1 in ALS mice

B. R. Roberts^{1,§}, N. K. H. Lim^{2,§}, E. J. McAllum^{2,§}, P. S. Donnelly^{3,4}, D. J. Hare^{1,5}, P. A. Doble⁵, B. J. Turner¹, K. A. Price², S. C. Lim^{3,4}, B. M. Paterson^{3,4}, J. L. Hickey^{3,4}, T. W. Rhoads^{6,7}, J. R. Williams^{6,7}, K. M. Kanninen², L. W. Hung^{1,4}, J. R. Liddell², A. Grubman², J. F. Monty⁸, R. M. Llanos⁸, D. R. Kramer⁹, J. F. B. Mercer⁸, A. I. Bush¹, C. L. Masters¹, J. A. Duce^{1,10}, Q. X. Li¹, J. S. Beckman^{6,7,11}, K. J. Barnham^{1,4,12}, A. R. White^{1,2}, and P. J. Crouch^{1,2,*}.

¹Florey Institute of Neuroscience and Mental Health, ²Department of Pathology, ³School of Chemistry, ⁴Bio21 Institute of Biotechnology and Molecular Biology, and ¹²Department of Pharmacology, The University of Melbourne, Parkville, Victoria, 3010, Australia.

⁵Elemental Bio-imaging Facility, and Department of Chemistry and Forensic Science, University of Technology Sydney, Broadway, New South Wales, 2007, Australia.

⁶Department of Biochemistry and Biophysics, ⁷Linus Pauling Institute, and ¹¹Environmental Health Sciences Centre, Oregon State University, Corvallis, OR 97331, USA.

⁸Centre for Cellular and Molecular Biology, School of Life and Environmental Sciences, Deakin University, Burwood, Victoria, 3125, Australia.

⁹ANU Medical School, ANU College of Medicine, Biology and the Environment, The Australian National University, Canberra, Australian Capital Territory, 0200, Australia.

¹⁰School of Molecular and Cellular Biology, University of Leeds, Leeds, LS2 9JT, United Kingdom.

* Address correspondence to: Dr Peter J. Crouch, Department of Pathology, The University of Melbourne, Parkville, Victoria 3010, Australia. E-mail: pjcrouch@unimelb.edu.au

§These authors contributed equally.

Conflict of Interest statement:

AIB is a paid consultant for Collaborative Medicinal Development LLC. Collaborative Medicinal Development LLC has licensed IP on this subject from the University of Melbourne, where the inventors are ARW, KJB and PSD.

Acknowledgements

This work was supported by funds from the Australian National Health and Medical Research Council [Project Grants 1005651 and 1061550]; the Motor Neuron Disease Research Institute of Australia; the Victorian Government's Operational Infrastructure Support Program; Bethlehem Griffiths Research Foundation; the CASS Foundation; the Australian Research Council; the National Academy of Finland; The Sigrid Juselius Foundation; and The University of Melbourne. Current address for KMK is AI Virtanen Institute for Molecular Sciences, University of Eastern Finland, Kuopio 70211, Finland. Current address for KAP is Department of Neuroscience, Icahn School of Medicine at Mount Sinai Hess Centre for Science and Medicine, 1470 Madison Ave, New York, NY 10029. Some of the samples used for histology were prepared by the Biomedical Sciences Histology Facility, The University of Melbourne

ABSTRACT

Mutations in the metallo-protein Cu/Zn-superoxide dismutase (SOD1) cause amyotrophic lateral sclerosis (ALS) in humans and an expression level-dependent phenotype in transgenic rodents. We show oral treatment with Cu^{II}(at-sm) increased the concentration of mutant SOD1 (SOD1G37R) in ALS model mice, but paradoxically improved locomotor function and survival of the mice. To determine why the mice with increased levels of mutant SOD1 had an improved phenotype we analyzed tissues by mass spectrometry. These analyses revealed most SOD1 in the spinal cord tissue of the SOD1G37R mice was Cu-deficient. Treating with Cu^{II}(at-sm) decreased the pool of Cu-deficient SOD1 and increased the pool of fully metallated holo-SOD1. Tracking isotopically enriched ⁶⁵Cu^{II}(at-sm) confirmed the increase in holo-SOD1 involved transfer of Cu from Cu^{II}(at-sm) to SOD1, suggesting the improved locomotor function and survival of the Cu^{II}(at-sm) treated SOD1G37R mice involved, at least in part, the compound's ability to improve the Cu content of the mutant SOD1. This was supported by improved survival of SOD1G37R mice that expressed the human gene for the Cu-uptake protein CTR1. Improving the metal content of mutant SOD1 *in vivo* with Cu^{II}(at-sm) did not decrease levels of mis-folded SOD1. These outcomes indicate the metal content of SOD1 may be a greater determinant of the protein's toxicity in mutant SOD1-associated forms of ALS than the mutations themselves. Improving the metal content of SOD1 therefore represents a valid therapeutic strategy for ALS caused by SOD1.

Keywords: Diacetyl-bis(4-methylthiosemicarbazonato)copper^{II} (Cu^{II}(at-sm)); amyotrophic lateral sclerosis (ALS); motor neuron disease (MND); copper; Cu/Zn superoxide dismutase (SOD1).

Abbreviations: Amyotrophic lateral sclerosis (ALS); motor neuron disease (MND); copper (Cu); Cu/Zn superoxide dismutase (SOD1); zinc (Zn); inductively coupled plasma mass spectrometry (ICPMS); liquid chromatography (LC); laser ablation (LA); standard suspension vehicle (SSV); copper transporter protein 1 (CTR1); copper chaperone for SOD1 (CCS); Cu-transporting ATPase 1 (ATP7A).

INTRODUCTION

Amyotrophic lateral sclerosis (ALS) is a fatal adult-onset disease in which motor neurons in the spinal cord and brain progressively deteriorate and die. Initial clinical symptoms of ALS are relatively mild, but inevitably progress to paralysis and premature death as the extent of motor neuron failure increases. Riluzole (trade name is Rilutek[®]) is the only approved treatment for ALS but its therapeutic effects are minimal. Treatment with riluzole provides an approximate three-month increase in patient survival and has no effect on the deterioration of muscle strength (Miller *et al.*, 1996; Bensimon *et al.*, 1994; Lacomblez *et al.*, 1996). The development of new treatment strategies for ALS is needed.

Approximately 90% of ALS cases are sporadic and 10% familial. Several genes are associated with the development of ALS, including *TARDBP* (Sreedharan *et al.*, 2008) and *C9ORF72* (DeJesus-Hernandez *et al.*, 2011; Renton *et al.*, 2011), but the gene for the ubiquitous antioxidant enzyme Cu/Zn-superoxide dismutase (SOD1) is the most widely studied to date and has provided the basis for the development of the most robust animal models of ALS. Over 100 different SOD1 mutations account for ~20% of familial ALS cases (Rosen *et al.*, 1993) and SOD1 mutations are also present in sporadic forms of the disease (Andersen *et al.*, 2003). Non-mutated, wild-type SOD1 is aberrantly metabolized in sporadic cases of ALS (Bosco *et al.*, 2010) and over-expression of wild-type SOD1 causes an ALS-like phenotype in mice that is comparable to the phenotype of ALS model mice caused by expression of mutant SOD1 (Graffmo *et al.*, 2013). Thus, the pathogenic role of SOD1 in ALS appears to extend beyond familial cases that involve SOD1 mutations.

Although oxidative damage is conspicuous in disease-affected tissues (Niebroj-Dobosz *et al.*, 2004), SOD1 mutations do not cause ALS by a loss of antioxidant function (Bruijn *et al.*, 1998). Motor neuron death in SOD1-associated forms of ALS therefore represents the consequences of a toxic gain-of-function in the mutant protein. Underscoring this, transgenic mice over-expressing mutant SOD1 develop an ALS-like phenotype that is proportional to expression level of the mutant SOD1. Higher levels of mutant SOD1 cause earlier disease onset, more severe disease symptoms, and more rapid disease progression (Gurney *et al.*, 1994; Wong *et al.*, 1995; Henriques *et al.*, 2010). However, despite the clear link between motor neuron death and disease symptoms in SOD1-associated forms of ALS, the fundamental basis of SOD1 toxicity in ALS is not fully understood. To address this, the present study examined spinal cord tissue collected from ALS model mice (SOD1G37R (Wong *et al.*, 1995)) that had been treated with the therapeutic agent diacetyl-bis(4-methylthiosemicarbazonato)copper^{II} (Cu^{II}(atm)). Given the ALS-like phenotype of these mice is driven by expression of the mutant SOD1, the aim of the study was to investigate the relationship between therapeutic activity of Cu^{II}(atm) and its effects on SOD1.

MATERIALS AND METHODS

SOD1G37R mice

SOD1G37R mice (Wong *et al.*, 1995) were used in this study. The effects of Cu^{II}(atsm) have been investigated previously in a G93A mouse model of ALS (Soon *et al.*, 2011). SOD1G37R mice purchased from The Jackson Laboratory (Bar Harbor, USA) and a colony maintained by breeding SOD1G37R-positive mice with non-transgenic C57BL/6 mice. Mice were housed in standard boxes (2-5 mice per box) with access to food and water *ad libitum*. Bedding for the boxes contained only saw dust and shredded paper with no other environmental enrichment. Light/dark cycles were 12h/12h. Mice were genotyped using tail snips obtained from the mice at the age of weaning (~3 weeks of age). Genotyping of all mice was determined using the commercial Extract-N-Amp™ Plant PCR Kit (Sigma), as per manufacturer's instructions to extract DNA from the sample tissue and to prepare samples for PCR (primers and cycling steps were obtained from The Jackson Laboratory website). The PCR product was run on a 1.7% agarose gel at 100 volts for 30 minutes and then imaged using the UVP BioDoc-It System (Pathtech).

All treatment groups contained approximately equal numbers of male and female mice. One cohort of mice was studied through to disease end-stage to obtain data on locomotor function. A second cohort of mice was culled at 24 weeks of age to collect tissues for biochemical and histological analyses. All mouse procedures were approved by Animal Ethics Committees of The University of Melbourne and the Mental Health Research Institute and complied with guidelines from the Australian National Health and Medical Research Council.

Treatment with Cu^{II}(atsm)

Cu^{II}(atsm) was synthesized as previously described (Blower *et al.*, 2003; Gingras *et al.*, 1962) and a suspension of the compound prepared daily in standard suspension vehicle (SSV; 0.9% (w/v) NaCl, 0.5% (w/v) Na-carboxymethylcellulose (medium viscosity), 0.5% (v/v) benzyl alcohol and 0.4% (v/v) tween-80). Cu^{II}(atsm) in SSV was administered daily to SOD1G37R mice or non-transgenic littermates by gavage, commencing at 40 days old, at a dose of 30 mg kg⁻¹ body weight day⁻¹. An equivalent volume of SSV was administered to sham treated mice. For some experiments mice were treated with ⁶⁵Cu^{II}(atsm) synthesized as per the standard Cu^{II}(atsm) except that the initial Cu source was ⁶⁵CuO (Trace Sciences International). In these experiments SOD1G37R mice were treated with ⁶⁵Cu^{II}(atsm), SSV, or Cu^{II}(atsm) by daily gavage for 2 weeks commencing when they were 12 weeks old. Mice in these experiments received Cu^{II}(atsm)/⁶⁵Cu^{II}(atsm) at 30 mg kg⁻¹ body weight.

hCTR1xSOD1G37R mice

The human *CTR1* coding sequence was amplified from human fibroblasts mRNA. The forward primer was used to introduce a Flag epitope just upstream from the start codon and the reverse primer was located just after the stop codon. The PCR product was cloned into pCMB336 (Ke *et al.*, 2006). A 4.1-kb *PvuI/StuI* fragment containing the CAG promoter, the *hCTR1* insert and a polyA signal was purified and used at 2 ng/μL for pronuclear microinjections in C57BL/6 females (Mouseworks, Monash University, Melbourne, Victoria, Australia). hCTR1 mice were genotyped by PCR of genomic DNA isolated from ear-notches (Viagen Biotech, Los Angeles, CA, USA). Detection of the *hCTR1* transgene and the endogenous *mCtr1* gene (as a control for the integrity of the extracted DNA) was carried out with the following primers: sense oligonucleotide *hCTR1* #1 (5'-TAAGTCACAAGTCAGCATTCGC) corresponding to the coding sequence of the *hCTR1* transgene and the antisense oligonucleotide SP6(2) from the vector (5'-GCTCTAGCATTTAGGTGACACTATAG); the sense oligonucleotide *mCtr1* #2 (5'-GCCAAGAGACCTTTGCTCTG) and the antisense oligonucleotide *mCtr1* #3 (5'-GCACCTTAATGTTGGGCTGT) corresponding to the 3' untranslated region of the endogenous *mCtr1* gene. C57BL/6 mice positive for the *hCTR1* transgene were backcrossed for two generations then brother/sister mating continued for a further seven generations. Double transgenic hCTR1xSOD1G37R mice were created by mating SOD1G37R hemizygotes with hCTR1 hemizygotes. Litters were genotyped for all possible genetic variants via PCR as described above.

hCTR1 expression was quantified using qRT-PCR methods described previously (Kanninen et al 2013 Biol Open) with all cDNA synthesis and qRT-PCR reagents from Life Technologies (Mulgrave, Australia). Briefly, RNA from non-transgenic (non-Tg) and transgenic *hCTR1* mouse spinal cord tissue (5 mg) was isolated and DNase-treated using the MagMAX™-96 Total RNA Isolation Kit. RNA concentrations were quantified using the Qubit® 2.0 Fluorometer then 200 ng RNA reverse transcribed using the High Capacity cDNA Reverse Transcription Kit. Primers for *hCTR1* were (GCTGGAAGAAGGCAGTGGTA and GGCCACGCCATAGAGTTTG) and for *mCtrl* were (TTCTTCAGGGTAGCTTCCGAGTA and CAACCTAGCGCAGGGATCT). Each 10 μ L reaction mix consisted of 300 nM primers, 5 μ L 2x Power SYBR Green Master Mix and 20 ng cDNA template. Duplicate reactions were performed using the LightCycler 480 (Roche) and the following conditions: 10 min at 95°C, followed by 45 cycles of 15 sec at 95°C, and 60°C for 60 sec. Cycle threshold (Ct) values were calculated as the lowest cycle number producing an exponential increase in PCR product amplification. Samples with Ct values below 30 were excluded from all analyses. The Δ Ct method was used to normalize *hCTR1* gene expression in each sample to expression of endogenous *mCtrl*. To assess whether *hCTR1* expression altered expression of endogenous *mCtrl* the Δ Ct method was used to normalize *mCtrl* gene expression in each sample to expression of endogenous *mActb*.

Locomotor function

Mice were tested for a locomotor function using the rotarod assay. Mice were trained for five days before data was recorded for analysis. During the data collection phase of the study the mice were tested on the rotarod twice a week. For SOD1G37R mice treated with Cu^{II}(atms), rotation speed of the rotarod was 25 rpm, and the time that each mouse could no longer stay on the rotarod (latency to fall) recorded, up to a maximum of 180 seconds. For mice in the *hCTR1*xSOD1G37R study, rotation speed of the rotarod accelerated from 4 to 40 rpm over 180 sec. Mice were placed on the rotarod twice during each testing period and only their maximum score recorded for analysis. Researchers performing the rotarod assay were blinded to the treatments.

Mouse survival

SOD1G37R mice eventually develop limb paralysis that prevents them from accessing food and water and individual mice in this study, regardless of treatment, were culled once they reached this stage. This stage was identified as the point at which individual mice had complete paralysis in at least one hind limb and were unable to right themselves within 15 sec after being laid down on their side. All survival data presented in this study therefore represent the age at which the mice reached this disease stage. Researchers who culled mice were blinded to the treatments and mouse genotype.

Tissue collection

Mice allocated to collecting tissues for biochemical analyses were killed when 24 weeks old. These mice were killed by intraperitoneal injection of PBS supplemented with ketamine (20 mg mL⁻¹) and xylazine (4 mg mL⁻¹), followed by transcardial perfusion with PBS containing 0.25% phosphatase inhibitor cocktail, 1% protease inhibitor (Roche) and 20 U mL⁻¹ heparin. After perfusion spinal cords and brains were removed. A small 5 mm section of the lumbar region of the spinal cord was removed and submersion fixed in 4% (v/v) paraformaldehyde and a similar lumbar section snap frozen on dry ice for subsequent mass spectrometry analyses. The remaining spinal cord material was snap frozen on dry ice for subsequent protein extraction and additional biochemical analyses.

SDS-PAGE

Spinal cords were homogenized using disposable polypropylene pestles for microfuge tubes (USA Scientific) in PBS supplemented with protease and phosphatase inhibitors (Sigma) then PBS-soluble and -insoluble fractions collected by centrifugation (16,000 x g, 30 min, 4°C). After determining protein content via the BCA Assay (Thermo Scientific) samples were prepared in sample buffer (62.6 mM Tris, 5% (v/v) glycerol, 2% (w/v) SDS, 0.0025% (w/v) bromophenol blue) then loaded onto 12% NuPAGE Novex Bis-Tris gels (Life Technologies) and electrophoresed at 175 V for 60 min in MES SDS running buffer (Life Technologies). Resolved proteins were transferred to PVDF membranes and western blotting performed as described previously (Donnelly

et al., 2012). Primary antibodies used were raised to detect human SOD1 (Abcam), mouse SOD1 (Abnova), and GAP43 (Novus Biologicals). Antibody immunoreactivity was detected using Enhanced Chemiluminescence (ECL Advance, GE Healthcare) and a FujiFilm LAS-3000 imager. Chemiluminescence images were saved as TIFF files and relative intensity of immunoreactivity determined using NIH ImageJ 1.38x software.

Native PAGE

PBS-soluble and -insoluble spinal cord extracts generated as above were prepared in native PAGE sample buffer (100 mM Tris, 10% (v/v) glycerol, 0.0025% (w/v) bromophenol blue, pH 8.6) then resolved on 12% tris-glycine gels (Life Technologies) at 125 V for 100 min in native tris-glycine running buffer (Life Technologies) prior to transferring to PVDF membranes as above. Membranes were probed using the primary antibodies A5C3, B8H10 and C4F6 (MediMabs). All three of these antibodies were generated to specifically detect mis-folded forms of human SOD1 but not natively folded wild-type SOD1 and data supporting this conformation-dependent immunoreactivity has been presented (Bosco *et al.*, 2010; Gros-Louis *et al.*, 2010). Immunoreactivity for these three antibodies was detected and quantified as described above.

Histology

Histology was performed based on methods previously described (Li *et al.*, 2006). Lumbar sections of mouse spinal cord were fixed in 4% (w/v) paraformaldehyde in PBS then embedded in wax and transverse 5 μ m or 20 μ m sections collected on glass slides. The 20 μ m sections were stained for nucleic acid material using cresyl violet (700 μ M in dH₂O, pH 3.8 with 1% acetic acid) then α -motor neurons in the ventral horn counted using light microscopy. Thirty-six sections from spinal cord regions spanning approximately 1800 μ m along the longitudinal plane of the spinal cord were counted per mouse. Data presented in Figure 1B represent the total number of α -motor neurons counted per mouse per ventral horn. To assess levels of Iba-1 and GFAP 5 μ m sections were quenched with peroxide, blocked with 20% (v/v) serum, then incubated with primary antibody (1:1000) overnight at 4°C. To assess levels of human SOD1 and mis-folded forms thereof proteinase-K treated 5 μ m sections were blocked with 20% (v/v) serum then incubated overnight at 4°C with primary antibodies to mis-folded SOD1 described above. Sections were developed using the universal LSAB[®]+HRP kit (Dako) as described by the manufacturer.

Protein oxidation

PBS-soluble tissue extracts prepared as above were analyzed for oxidatively modified proteins using the Oxyblot Protein Oxidation Detection Kit (Millipore). Oxidatively modified proteins were derivatized as per kit instructions then loaded onto 12% tris-glycine gels (Life Technologies) prior to transferring to PVDF membranes as above. Membranes were probed for derivatized proteins using kit antibodies and oxidatively modified proteins detected via chemiluminescence as above.

SOD activity assay

SOD activity gels were performed as previously described (Soon *et al.*, 2011). Briefly, soluble samples collected from spinal cord tissue were diluted in native sample buffer and 1 μ g protein loaded onto a native 12% tris-glycine gel. After electrophoresis gels were then immersed in nitroblue tetrazolium then developed with tetramethylethylenediamine and riboflavin in KH₂PO₄ buffer.

Mass spectrometric quantification

The metal status and total SOD concentration was determined as described (Rhoads *et al.*, 2011) with the following modifications. Mouse tissues were dissected frozen, on a plastic dissection plate placed on a block of dry ice to maintain a sub-zero temperature. For spinal cords, 1-2 mm thick transverse sections were cut with a razor blade, laid flat on the dissection plate and 0.3 mm diameter punches of either dorsal or ventral grey matter (300 micron biopsy punch, Zivic Instruments) were taken. The tissue was expelled with air from the punch onto a tared aluminium weigh boat (VWR) and then weighed to the nearest microgram using an analytical balance (CAHN 25 automatic electrobalance). Punch weights ranged between 90-200 μ g. The punch was then mixed with 5 μ L 10 mM ammonium acetate pH 5.1, containing 500 nM bovine SOD as an internal standard. The supernatant was then bound to an equilibrated C₄ Ziptip (Millipore) and desalted by aspirating with

10 μL of deionized water repeated six times. The point of the Ziptip was then pressed into PEEK tubing leading to the electrospray ionization source of a LTQ-FT Ultra MS (ThermoScientific, USA) with an electrospray ionization interface in positive-ion mode. A second piece of PEEK tubing coming from the HPLC pump was inserted into the rear of the Ziptip and the tip was then perfused with a mobile phase of 30% (v/v) acetonitrile/water with 100 μM formic acid (at 30 mL min^{-1}). The elution of SOD occurred over 2-3 min, after which time the total ion count returned to baseline. Integration and quantitation of SOD was done as described previously (Rhoads *et al.*, 2011; Rhoads *et al.*, 2013).

Size exclusion chromatography inductively couple plasma mass spectrometry (LC-ICPMS)

LC-ICPMS was carried out using a HPLC (1200, Agilent, USA) equipped with binary pumps, in line degasser, thermostat controlled column compartment, variable wavelength detector and temperature control autosampler. The HPLC was directly connected to Miramist Teflon nebulizer with PEEK tubing. An Agilent 7700 series ICPMS instrument was used as a multielemental detector and was operated in He mode (4.3 mL min^{-1}) under routine multi-elemental operating conditions. Samples were chromatographically separated with a BioSEC3 size exclusion column (4.6 mm x 300 mm, 300 \AA , Agilent, USA) with 200 mM ammonium nitrate pH 8.0 at a flow rate of 0.4 mL min^{-1} (145 cm hour^{-1} , 30 $^{\circ}\text{C}$). The size exclusion column was calibrated using the following molecular weight standards and elution volume was monitored both by absorbance (280 nm) and by ICPMS (mass of each standard, element detected by ICPMS, and source of standard are shown in parentheses); thyroglobin (667 kDa; I; GE), ferritin (440 kDa; Fe; GE), catalase (232 kDa; Fe; GE), albumin (64 kDa; Fe, Cu, Zn; GE), bovine SOD1 (32 kDa; Cu, Zn; Sigma), vitamin B₁₂ (1.2 kDa; Co; Sigma) integration time for each element was 0.2 s. A standard curve of SOD1 (bovine, Sigma) was also determined by measuring the amount of SOD protein ($\epsilon_{258} = 10,300 \text{ M}^{-1}\text{cm}^{-1}$) and the total amount of Cu and Zn determined by bulk measure ICPMS. The standard curve was linear over the range of 1-1000 pmol SOD injected on column ($r^2 > 0.98$). PBS-soluble spinal cord extracts (prepared as above) containing 200 μg of total protein were injected on column ($\sim 20 \mu\text{L}$ injections) and developed for 1.6 column volumes (8 mL).

Laser ablation inductively couple plasma mass spectrometry (LA-ICPMS)

LA-ICPMS imaging mass spectrometry was performed on paraformaldehyde fixed spinal cord transverse sections as previously described (Lear *et al.*, 2012; Hare *et al.*, 2012). Imaging mass spectrometry is a relatively new analytical science that combines discrete solid sampling with mass specific detection. LA-ICPMS employs high-energy laser pulses to provide a source of particles for inorganic mass spectrometry, allowing spatial profiling of trace metals directly in solid samples. Quantitative images depicting the spatial distribution of metals in tissue sections are produced by rastering the laser beam across the tissue surface.

Statistical analyses

The Kolmogorov-Smirnov test for normality (with Dallal-Wilkinson-Lilliefors P value) was applied to all data sets to test for Gaussian distribution. Normally distributed data were analyzed using the unpaired t test when comparing the mean of two data sets or a two-way ANOVA (with Bonferroni post tests). Data that did not fit Gaussian distribution were analyzed using the Mann-Whitney test when comparing the mean of two data sets. Statistical significance of mouse survival data was determined using the Log-rank (Mantel-Cox) test. Statistical significance of locomotor function data was determined using a two-way repeat measures ANOVA.

RESULTS

Cu^{II}(atsm) is protective in SOD1G37R mice

Daily treatment with Cu^{II}(atsm) improves locomotor function and survival of SOD1G37R mice in a dose-dependent manner without affecting locomotor function of non-transgenic littermates (McAllum *et al.*, 2013) (Figure 1A). The observed therapeutic outcomes involve broad protection against the toxic effects of mutant SOD1 as treatment with Cu^{II}(atsm) preserved the number of α -motor neurons in the spinal cord (Figure 1B), decreased levels of oxidatively modified proteins (Figure 1C), decreased the abundance of GFAP immunoreactive cells (astrocytes) within spinal cord grey matter, and decreased the abundance of activated microglia (Figure 1D). All biochemical and histological analyses were performed on tissues collected at the mid-symptom age of 24 weeks, as indicated by vertical dashed line in Figure 1A. Relatively modest changes in α -motor neuron numbers are consistent with the severity of disease symptoms at this age (Feeney *et al.*, 2001).

Cu^{II}(atsm) increases levels of mutant SOD1 *in vivo* by increasing the protein's Cu content

We examined whether therapeutic activity of Cu^{II}(atsm) was related to effects on levels of mutant SOD1. Surprisingly, an increase in the mutant form of SOD1 was detected in the spinal cords of Cu^{II}(atsm) treated mice. This was evident via western blot (Figure 2A,B) and histology (Figure 2C). Endogenous, wild-type mouse SOD1 was not affected by the Cu^{II}(atsm) treatment (Figure 2A,B). A substantial pool of metal-deficient SOD1 (i.e. where each monomer equivalent of SOD1 contains one Cu ion or one Zn ion, but not both) was decreased by the Cu^{II}(atsm) treatment, whereas the increase in total SOD1 was driven by an increase in the pool of fully metallated holo-SOD1 (Figure 2D). Conversion of metal-deficient SOD1 to holo-SOD1 appeared to be driven by delivery of Cu to the mutant protein as Cu-deficient SOD1 was the only form of metal-deficient SOD1 that decreased (Figure 2E) as indicated by the strong correlation between metal-deficient SOD1 and Cu-deficient SOD1 (Figure 2F). There was no correlation between metal-deficient SOD1 and Zn-deficient SOD1 ($R^2=0.003$, $P=0.8$, data not shown). Supporting an increase in the amount of SOD1 that contained Cu, SOD activity was increased in the spinal cords of Cu^{II}(atsm) treated SOD1G37R mice (Figure 2G).

LA-ICPMS data (Figure 3) showed that oral treatment with Cu^{II}(atsm) increased the Cu content of the spinal cords of non-transgenic mice 2.2-fold (Figure 3) and this is consistent with data that show orally administered Cu^{II}(atsm) penetrates CNS tissue (Hung *et al.*, 2012; Soon *et al.*, 2011). The increase in spinal cord Cu was more pronounced in SOD1G37R mice (Figure 3B) indicating the Cu^{II}(atsm) had elevated penetration of CNS tissue in SOD1G37R mice or that the compound was selectively retained and/or metabolized within the CNS tissue of SOD1G37R mice. Treating with Cu^{II}(atsm) also increased overall levels of Zn in spinal cords of SOD1G37R mice, but unlike Cu the increase in Zn was not evident in non-transgenic mice (Figure 3). Fe levels (Figure 3) and Mn levels (not shown) were not changed.

To gain further information on the Cu^{II}(atsm)-induced changes within the pool of holo-SOD1G37R and its associated metal ions Cu and Zn, we performed size exclusion liquid chromatography coupled to inductively coupled plasma mass spectrometry (LC-ICPMS). This metalloproteomic approach revealed that Cu and Zn were both increased in SOD1 by the Cu^{II}(atsm) treatment (Figure 4A,B). The ratio of Cu:Zn within the SOD1G37R calculated from these LC-ICPMS data confirmed that SOD1G37R in spinal cords of vehicle treated mice was relatively Cu-deficient (Figure 4C). The Cu^{II}(atsm)-induced increase in the SOD1G37R Cu:Zn ratio was consistent with the LA-ICPMS data (Figure 3) which showed Cu^{II}(atsm) had a greater effect on Cu levels in the spinal cord compared to Zn.

Data in Figures 3 and 4 collectively indicate treatment with Cu^{II}(atsm) increases the total levels of Cu and Zn and the amount of holo-mutant SOD1 within the spinal cord tissue. Cu^{II}(atsm) has the capacity to increase levels of bio-available Cu and Zn in cells *in vitro* (Donnelly *et al.*, 2012). This indicates the increase in Cu in the mutant SOD1 (Figure 4A) involved transfer of Cu from Cu^{II}(atsm) to SOD1, and that the increase in Zn occurs via an indirect mechanism. To probe further the *in vivo* transfer of Cu from Cu^{II}(atsm) to mutant SOD1 mice were treated with Cu^{II}(atsm) isotopically enriched with ⁶⁵Cu. This naturally occurring isotope is less abundant than

the predominant ^{63}Cu isotope, with the natural ratio 0.45:1 (^{65}Cu : ^{63}Cu). LC-ICPMS analysis of spinal cord tissue demonstrated an increase in abundance of ^{65}Cu in the SOD1 of $^{65}\text{Cu}^{\text{II}}$ (atsm) treated mice (Figure 4D), indicating transfer of Cu from Cu^{II} (atsm) to the SOD1. Based on a total spinal cord wet weight of ~50 mg the data in Figure 4D equate to *ca.* 2% of the total Cu delivered orally to the mice as Cu^{II} (atsm) being transferred to SOD1 in the spinal cord.

Treatment with Cu^{II} (atsm) did not decrease levels of mis-folded SOD1

Sub-optimal metal content of SOD1 can promote SOD1 mis-folding and aggregation (Lynch *et al.*, 2004; Rumfeldt *et al.*, 2009; Ip *et al.*, 2011) and mis-folded and aggregated SOD1 is a consistent feature of ALS (Bruijn *et al.*, 1998; Chattopadhyay and Valentine, 2009; Furukawa *et al.*, 2006; Prudencio *et al.*, 2009; Wang *et al.*, 2008), including sporadic ALS (Bosco *et al.*, 2010). Given Cu^{II} (atsm) improved the metal content of the mutant SOD1 (Figure 3) the levels of mis-folded SOD1 in the spinal cords of Cu^{II} (atsm) treated SOD1G37R mice were assessed using three antibodies raised against mis-folded SOD1 (Bosco *et al.*, 2010; Gros-Louis *et al.*, 2010). Mis-folded SOD1 was readily detectable in the soluble fraction of spinal cords from SOD1G37R mice but the Cu^{II} (atsm) treatment did not significantly alter its abundance (Figure 5A-C). Results for all three antibodies trended towards an increase in mis-folded SOD1 in the soluble fraction in the Cu^{II} (atsm) treated mice and this was supported by histology data (Figure 5D). Consistent with previous reports (Brotherton *et al.*, 2012; Rakhit *et al.*, 2007; Zetterstrom *et al.*, 2007), levels of mis-folded SOD1 were low or non-detectable in the insoluble fraction (Figure 5A-C).

Increasing spinal cord Cu via the Cu uptake transporter CTR1 improved survival of SOD1G37R mice

To help assess significance of Cu delivery in the protective activity of Cu^{II} (atsm) in SOD1G37R mice we aimed to increase spinal cord Cu levels via an alternate method. This was achieved by crossing SOD1G37R mice with mice that express the gene for the human Cu uptake transporter CTR1. Expression of *hCTR1* in the spinal cord tissue (Figure 6A) induced a 19% increase in spinal cord Cu levels without altering levels of Zn or Fe (Figure 6B). Expression of endogenous *mCtrl* was not altered by expression of *hCTR1* (Figure 6A). The elevation in spinal cord Cu translated into a modest (but statistically insignificant) improvement in locomotor function (Figure 6C) and a significant ($P=0.006$) 12% increase in median survival of SOD1G37R mice (Figure 6D).

DISCUSSION

Early studies showed that higher levels of expressed mutant SOD1 correlate with more rapid onset and progression of disease symptoms in ALS model mice (Wong et al., 1995; Dal Canto and Gurney, 1997; Gurney et al., 1994). This correlation is substantiated by delayed symptoms in ALS mice due to decreased mutant SOD1 levels (Henriques et al., 2010; Ralph *et al.*, 2005; Urushitani *et al.*, 2007). Because of this clear apparent relationship between mutant SOD1 levels and phenotype of the mice, we measured SOD1 in spinal cords of Cu^{II}(at-sm)-treated SOD1G37R mice. Despite the treatment improving mouse locomotor function and survival (McAllum *et al.*, 2013) (Figure 1A) we found Cu^{II}(at-sm) significantly increased the mutant protein *in vivo* (Figure 2), thereby disproving the assertion that the phenotype of mutant SOD1 mice is proportional to levels of the mutant protein.

Mass spectrometry analyses indicated Cu^{II}(at-sm) promoted conversion of metal-deficient SOD1 to holo-SOD1 (Figure 2D-F) via *in vivo* transfer of Cu from Cu^{II}(at-sm) to the mutant SOD1: the Cu content of SOD1 was increased (Figure 4A) and ⁶⁵Cu from orally administered ⁶⁵Cu^{II}(at-sm) was recovered in spinal cord SOD1 (Figure 4D). These outcomes are consistent with high stability of holo-SOD1 (Forman and Fridovich, 1973) regardless of the presence of ALS-associated mutations (Banci *et al.*, 2007) and support *in vitro* studies that indicate SOD1 toxicity can be prevented by improving the protein's metallation state (Estevez *et al.*, 1999). These outcomes indicate the metal content of SOD1 may be a greater determinant of the protein's toxicity in mutant SOD1-associated forms of ALS than the mutations themselves.

A number of mechanisms have been proposed to explain how an altered metal content of SOD1 may cause ALS. One of these involves pro-oxidant gain-of-function for Zn-deficient SOD1 (Crow *et al.*, 1997). This proposed toxic gain-of-function requires retention of Cu in Zn-deficient SOD1 as it is the redox activity of Cu that catalyzes production of reactive oxygen and nitrogen species (Crow *et al.*, 1997; Estevez *et al.*, 1999; Sahawneh *et al.*, 2010). This toxic mechanism of action is supported by a number of lines of evidence (Roberts *et al.*, 2007; Sahawneh *et al.*, 2010; Estevez *et al.*, 1999), and although the Zn-deficient pool of SOD1 only accounts for <1% of SOD1 in the SOD1G37R (Figure 2E) our data show the concentration of Zn-deficient SOD1 in spinal cord tissue is higher than concentrations that induce motor neuron toxicity *in vitro* (Sahawneh *et al.*, 2010). However, SOD1 mice in which all four Cu-coordinating histidine residues in the mutant SOD1 are removed have been developed and these mice still develop ALS-like symptoms (Wang *et al.*, 2003). While the phenotype of these "quad mutant" mice does not exclude Cu-mediated SOD1 toxicity occurring via Cu that binds to the SOD1 Zn-binding site (Valentine *et al.*, 1979), the absence of any significant changes to the pool of Zn-deficient SOD1 in Cu^{II}(at-sm)-treated SOD1G37R mice indicates the modulation of Zn-deficient SOD1 is not part of the therapeutic mechanism of action for Cu^{II}(at-sm).

Metal-free SOD1 readily mis-folds and aggregates (Lynch *et al.*, 2004; Rumpfheldt *et al.*, 2009; Arnesano *et al.*, 2004; Durazo *et al.*, 2009; Furukawa *et al.*, 2008; Tiwari *et al.*, 2009), thus potentially giving rise to the SOD1 aggregates present in some forms of ALS. Significantly, ALS-causing SOD1 mutations promote SOD1 mis-folding via a pathway in which the mutant SOD1 preferentially loses Cu (Ip *et al.*, 2011), and restoration of the protein's full metal complement makes it relatively indistinguishable from holo wild-type SOD1 (Banci *et al.*, 2007). However, despite this relationship between Cu-deficiency and SOD1 mis-folding, preventing the formation of mis-folded SOD1 is not the mechanism through which Cu^{II}(at-sm) improved the locomotor function and survival of SOD1G37R mice, as none of the antibodies used to assess levels of mis-folded SOD1 revealed a decrease in the pool of mis-folded SOD1 (Figure 5A-D). In fact, all three antibodies indicated the soluble pool of mis-folded SOD1 increased in equilibrium with the total pool of SOD1 (Figure 2A). Previous studies have shown decreasing levels of mis-folded SOD1 improves survival and locomotor function of mutant SOD1 mice, suppresses inflammatory responses, and protects spinal cord motor neurons (Gros-Louis *et al.*, 2010; Liu *et al.*, 2012), outcomes that were all detected in Cu^{II}(at-sm)-treated SOD1G37R mice (Figure 1). Without precluding potential contribution of methodological differences between the studies, these apparent

disparate outcomes may indicate that SOD1-mediated dysfunction in ALS is not due to a single toxic species of SOD1, and that mis-folded SOD1 only contributes partially to decreased neuron functionality in ALS. Supporting this, none of the therapeutic interventions tested to date, including $\text{Cu}^{\text{II}}(\text{atsm})$, has completely prevented death or locomotor deficits in ALS model mice.

SOD1 that is relatively Cu-deficient and Zn-replete has been reported in the spinal cords of ALS model mice (Lelie *et al.*, 2011) and is supported by data in Figure 4C. Our observation that Cu-deficient SOD1 was the only pool of SOD1 decreased by $\text{Cu}^{\text{II}}(\text{atsm})$ indicates that if the phenotype of the SOD1G37R mice is driven solely by mutant SOD1, increasing bio-available Cu in the spinal cord is beneficial because it decreases abundance of the Cu-deficient pool of SOD1. This is supported by data that show over-expression of CTR1 improves survival of SOD1G37R mice (Figure 6) and by data that show Cu administered orally as $\text{Cu}^{\text{II}}(\text{atsm})$ is recovered in spinal cord SOD1 (Figure 4D). However, modulating levels of spinal cord Cu to treat mutant SOD1 mice has been investigated previously, and the outcomes often indicate decreasing Cu is beneficial. Treating with ammonium tetrathiomolybdate for example is effective in mutant SOD1 mice via a mechanism proposed to involve attenuation of the Cu dyshomeostasis caused by mutant SOD1, and is supported by data that show the treatment decreases levels of spinal cord Cu and removes Cu from the SOD1 active site (Tokuda *et al.*, 2013; Tokuda *et al.*, 2008). Conversely, treating mutant SOD1 rats with pyrrolidine dithiocarbamate, a compound capable of increasing Cu in central nervous system tissue (Malm *et al.*, 2007), accelerated the ALS-like phenotype of mutant SOD1 rats (Ahtoniemi *et al.*, 2007). Targeting metal ion homeostasis therefore has good *in vivo* support as a strategy for treating ALS, but the interpretation of outcomes from studies that use notional metal chelating agents as opposed to metal delivery agents is complicated by incomplete understanding of the activity of these compounds at the cellular level as recently reviewed (Crouch and Barnham, 2012).

Other studies have attempted to modulate disease symptoms in mutant SOD1 mice by genetic modification of Cu transporters and chaperones. The first of these utilized mice that had no Cu chaperone for SOD1 (CCS), a cellular chaperone that delivers intracellular Cu to SOD1. The SOD1/CCS^{-/-} mice had decreased Cu levels in SOD1 but did not have an altered phenotype, thus generating the conclusion that the Cu content of mutant SOD1 did not contribute to SOD1 toxicity *in vivo* (Subramaniam *et al.*, 2002). This interpretation has been criticized (Beckman *et al.*, 2002; Kiaei *et al.*, 2004) based on data that show CCS is not the only chaperone that delivers Cu to SOD1 (Carroll *et al.*, 2004). By contrast, mice that express mutant SOD1 and a dysfunctional Cu-transporting ATPase 1 (ATP7A) displayed increased survival and locomotor function relative to mutant SOD1 mice with functional ATP7A, and it was shown expression of the dysfunctional ATP7A significantly decreased global levels of spinal cord Cu (Kiaei *et al.*, 2004). Also, over-expression of CCS in mutant SOD1 mice dramatically accelerates disease onset and premature death (Son *et al.*, 2007). Data from the CTR1 over-expressing mice (Figure 6) support outcomes from our $\text{Cu}^{\text{II}}(\text{atsm})$ studies, but on face-value appear to oppose outcomes from mice with altered CCS or ATP7A functionality. Fundamental differences between the Cu transporters and chaperones modulated in these studies and their likely differing effects with respect to metallo-proteins other than SOD1 will have contributed to these apparent opposing outcomes. If anything, these studies demonstrate the often-underestimated complexity of biometal metabolism. More information on how the metal content of SOD1 and other cupro-proteins is changed in these models is needed to reconcile these disparate outcomes.

While the definitive roles for altered Cu and Zn homeostasis in the toxic gain-of-function of SOD1 continue to be debated, the sub-optimal metal content of SOD1 is nonetheless emerging as an important factor with excellent potential for therapeutic intervention. Our data indicate $\text{Cu}^{\text{II}}(\text{atsm})$ may mediate its protective effects, at least in part, by delivering Cu to Cu-deficient SOD1 thereby converting it to stable, non-toxic holo-SOD1. This therapeutic strategy does not preclude the potential benefits of removing Cu from, for example, Zn-deficient SOD1 in order to prevent a pro-oxidant gain-of-function. When considered with outcomes from previous studies our data support the conclusion that at least part the toxic gain-of-function of SOD1 resides in a metal-

deficient intermediate, and that driving the protein towards holo-SOD1 via metal delivery or towards apo-SOD1 via sequestration appears to have comparable therapeutic potential (Figure 7). Our data add support to the strengthening hypothesis that combination therapy is likely to provide the best outcomes for ALS.

REFERENCES

- Ahtoniemi T, Goldsteins G, Keksa-Goldsteine V, Malm T, Kanninen K, Salminen A, Koistinaho J (2007) Pyrrolidine dithiocarbamate inhibits induction of immunoproteasome and decreases survival in a rat model of amyotrophic lateral sclerosis. *Mol Pharmacol* 71:30-37.
- Andersen PM, Sims KB, Xin WW, Kiely R, O'Neill G, Ravits J, Pioro E, Harati Y, Brower RD, Levine JS, Heinicke HU, Seltzer W, Boss M, Brown RH, Jr. (2003) Sixteen novel mutations in the Cu/Zn superoxide dismutase gene in amyotrophic lateral sclerosis: a decade of discoveries, defects and disputes. *Amyotroph Lateral Scler Other Motor Neuron Disord* 4:62-73.
- Arnesano F, Banci L, Bertini I, Martinelli M, Furukawa Y, O'Halloran TV (2004) The unusually stable quaternary structure of human Cu,Zn-superoxide dismutase 1 is controlled by both metal occupancy and disulfide status. *J Biol Chem* 279:47998-48003.
- Banci L, Bertini I, D'Amelio N, Libralesso E, Turano P, Valentine JS (2007) Metalation of the amyotrophic lateral sclerosis mutant glycine 37 to arginine superoxide dismutase (SOD1) apoprotein restores its structural and dynamical properties in solution to those of metalated wild-type SOD1. *Biochemistry* 46:9953-9962.
- Beckman JS, Esetvez AG, Barbeito L, Crow JP (2002) CCS knockout mice establish an alternative source of copper for SOD in ALS. *Free Radic Biol Med* 33:1433-1435.
- Bensimon G, Lacomblez L, Meininger V (1994) A controlled trial of riluzole in amyotrophic lateral sclerosis. ALS/Riluzole Study Group. *N Engl J Med* 330:585-591.
- Blower PJ, Castle TC, Cowley AR, Dilworth JR, Donnelly PS, Labisbal E, Sowrey FE, Teat SJ, Went MJ (2003) Structural trends in copper(II) bis(thiosemicarbazone) radiopharmaceuticals. *Dalton Trans* 4416-4425.
- Bosco DA, Morfini G, Karabacak NM, Song Y, Gros-Louis F, Pasinelli P, Goolsby H, Fontaine BA, Lemay N, McKenna-Yasek D, Frosch MP, Agar JN, Julien JP, Brady ST, Brown RH, Jr. (2010) Wild-type and mutant SOD1 share an aberrant conformation and a common pathogenic pathway in ALS. *Nat Neurosci* 13:1396-1403.
- Brotherton TE, Li Y, Cooper D, Gearing M, Julien JP, Rothstein JD, Boylan K, Glass JD (2012) Localization of a toxic form of superoxide dismutase 1 protein to pathologically affected tissues in familial ALS. *Proc Natl Acad Sci U S A* 109:5505-5510.
- Brujin LI, Houseweart MK, Kato S, Anderson KL, Anderson SD, Ohama E, Reaume AG, Scott RW, Cleveland DW (1998) Aggregation and motor neuron toxicity of an ALS-linked SOD1 mutant independent from wild-type SOD1. *Science* 281:1851-1854.
- Carroll MC, Girouard JB, Ulloa JL, Subramaniam JR, Wong PC, Valentine JS, Culotta VC (2004) Mechanisms for activating Cu- and Zn-containing superoxide dismutase in the absence of the CCS Cu chaperone. *Proc Natl Acad Sci U S A* 101:5964-5969.
- Chattopadhyay M, Valentine JS (2009) Aggregation of copper-zinc superoxide dismutase in familial and sporadic ALS. *Antiox Redox Signal* 11:1603-1614.
- Crouch PJ, Barnham KJ (2012) Therapeutic redistribution of metal ions to treat Alzheimer's disease. *Acc Chem Res* 45:1604-1611.
- Crow JP, Sampson JB, Zhuang Y, Thompson JA, Beckman JS (1997) Decreased zinc affinity of amyotrophic lateral sclerosis-associated superoxide dismutase mutants leads to enhanced catalysis of tyrosine nitration by peroxynitrite. *J Neurochem* 69:1936-1944.
- Dal Canto MC, Gurney ME (1997) A low expressor line of transgenic mice carrying a mutant human Cu,Zn superoxide dismutase (SOD1) gene develops pathological changes that most closely resemble those in human amyotrophic lateral sclerosis. *Acta Neuropathol* 93:537-550.
- DeJesus-Hernandez M et al. (2011) Expanded GGGGCC hexanucleotide repeat in noncoding region of C9ORF72 causes chromosome 9p-linked FTD and ALS. *Neuron* 72:245-256.
- Donnelly PS, Liddell JR, Lim S, Paterson BM, Cater MA, Savva MS, Mot AI, James JL, Trounce IA, White AR, Crouch PJ (2012) An impaired mitochondrial electron transport chain

- increases retention of the hypoxia imaging agent diacetylbis(4-methylthiosemicarbazonato)copperII. *Proc Natl Acad Sci USA* 109:47-52.
- Durazo A, Shaw BF, Chattopadhyay M, Faull KF, Nersissian AM, Valentine JS, Whitelegge JP (2009) Metal-free superoxide dismutase-1 and three different amyotrophic lateral sclerosis variants share a similar partially unfolded beta-barrel at physiological temperature. *J Biol Chem* 284:34382-34389.
- Estevez AG, Crow JP, Sampson JB, Reiter C, Zhuang Y, Richardson GJ, Tarpey MM, Barbeito L, Beckman JS (1999) Induction of nitric oxide-dependent apoptosis in motor neurons by zinc-deficient superoxide dismutase. *Science* 286:2498-2500.
- Feeney SJ, McKelvie PA, Austin L, Jean-Francois MJ, Kapsa R, Tombs SM, Byrne E (2001) Presymptomatic motor neuron loss and reactive astrocytosis in the SOD1 mouse model of amyotrophic lateral sclerosis. *Muscle Nerve* 24:1510-1519.
- Forman HJ, Fridovich I (1973) On the stability of bovine superoxide dismutase. The effects of metals. *J Biol Chem* 248:2645-2649.
- Furukawa Y, Fu R, Deng HX, Siddique T, O'Halloran TV (2006) Disulfide cross-linked protein represents a significant fraction of ALS-associated Cu, Zn-superoxide dismutase aggregates in spinal cords of model mice. *Proc Natl Acad Sci U S A* 103:7148-7153.
- Furukawa Y, Kaneko K, Yamanaka K, O'Halloran TV, Nukina N (2008) Complete loss of post-translational modifications triggers fibrillar aggregation of SOD1 in the familial form of amyotrophic lateral sclerosis. *J Biol Chem* 283:24167-24176.
- Gingras BA, Suprunchuk T, Bayley CH (1962) The preparation of some thiosemicarbazones and their copper complexes: Part III. *Can J Chem* 40:1053-1059.
- Graffmo KS, Forsberg K, Bergh J, Birve A, Zetterstrom P, Andersen PM, Marklund SL, Brannstrom T (2013) Expression of wild-type human superoxide dismutase-1 in mice causes amyotrophic lateral sclerosis. *Hum Mol Genet* 22:51-60.
- Gros-Louis F, Soucy G, Lariviere R, Julien JP (2010) Intracerebroventricular infusion of monoclonal antibody or its derived Fab fragment against misfolded forms of SOD1 mutant delays mortality in a mouse model of ALS. *J Neurochem* 113:1188-1199.
- Gurney ME, Pu H, Chiu AY, Dal Canto MC, Polchow CY, Alexander DD, Caliendo J, Hentati A, Kwon YW, Deng HX, et al. (1994) Motor neuron degeneration in mice that express a human Cu,Zn superoxide dismutase mutation. *Science* 264:1772-1775.
- Hare D, Austin C, Doble P (2012) Quantification strategies for elemental imaging of biological samples using laser ablation-inductively coupled plasma-mass spectrometry. *Analyst* 137:1527-1537.
- Henriques A, Pitzer C, Schneider A (2010) Characterization of a novel SOD-1(G93A) transgenic mouse line with very decelerated disease development. *PLoS One* 5:e15445.
- Hung LW et al. (2012) The hypoxia imaging agent CuII(atSm) is neuroprotective and improves motor and cognitive functions in multiple animal models of Parkinson's disease. *J Exp Med* 209:837-854.
- Ip P, Mulligan VK, Chakrabartty A (2011) ALS-causing SOD1 mutations promote production of copper-deficient misfolded species. *J Mol Biol* 409:839-852.
- Ke BX, Llanos RM, Wright M, Deal Y, Mercer JF (2006) Alteration of copper physiology in mice overexpressing the human Menkes protein ATP7A. *Am J Physiol Regul Integr Comp Physiol* 290:R1460-1467.
- Kiaei M, Bush AI, Morrison BM, Morrison JH, Cherny RA, Volitakis I, Beal MF, Gordon JW (2004) Genetically decreased spinal cord copper concentration prolongs life in a transgenic mouse model of amyotrophic lateral sclerosis. *J Neurosci* 24:7945-7950.
- Lacomblez L, Bensimon G, Leigh PN, Guillet P, Meininger V (1996) Dose-ranging study of riluzole in amyotrophic lateral sclerosis. Amyotrophic Lateral Sclerosis/Riluzole Study Group II. *Lancet* 347:1425-1431.

- Lear J, Hare DJ, Fryer F, Adlard PA, Finkelstein DI, Doble PA (2012) High-resolution elemental bioimaging of Ca, Mn, Fe, Co, Cu, and Zn employing LA-ICP-MS and hydrogen reaction gas. *Anal Chem* 84:6707-6714.
- Lelie HL, Liba A, Bourassa MW, Chattopadhyay M, Chan PK, Gralla EB, Miller LM, Borchelt DR, Valentine JS, Whitelegge JP (2011) Copper and zinc metallation status of copper-zinc superoxide dismutase from amyotrophic lateral sclerosis transgenic mice. *J Biol Chem* 286:2795-2806.
- Li QX, Mok SS, Laughton KM, McLean CA, Volitakis I, Cherny RA, Cheung NS, White AR, Masters CL (2006) Overexpression of Abeta is associated with acceleration of onset of motor impairment and superoxide dismutase 1 aggregation in an amyotrophic lateral sclerosis mouse model. *Aging Cell* 5:153-165.
- Liu HN, Tjostheim S, Dasilva K, Taylor D, Zhao B, Rakhit R, Brown M, Chakrabartty A, McLaurin J, Robertson J (2012) Targeting of monomer/misfolded SOD1 as a therapeutic strategy for amyotrophic lateral sclerosis. *J Neurosci* 32:8791-8799.
- Lynch SM, Boswell SA, Colon W (2004) Kinetic stability of Cu/Zn superoxide dismutase is dependent on its metal ligands: implications for ALS. *Biochemistry* 43:16525-16531.
- Malm TM, Iivonen H, Goldsteins G, Keksa-Goldsteine V, Ahtoniemi T, Kanninen K, Salminen A, Auriola S, Van Groen T, Tanila H, Koistinaho J (2007) Pyrrolidine dithiocarbamate activates Akt and improves spatial learning in APP/PS1 mice without affecting beta-amyloid burden. *J Neurosci* 27:3712-3721.
- McAllum EJ, Lim NKH, Hickey JL, Paterson BM, Donnelly PS, Li QX, Barnham KJ, White AR, Crouch PJ (2013) Therapeutic effects of Cu^{II}(atsm) in the SOD1G37R mouse model of amyotrophic lateral sclerosis. *Amyotroph Lateral Scler Fronto Degen* 14:586-590.
- Miller RG, Bouchard JP, Duquette P, Eisen A, Gelinas D, Harati Y, Munsat TL, Powe L, Rothstein J, Salzman P, Sufit RL (1996) Clinical trials of riluzole in patients with ALS. ALS/Riluzole Study Group-II. *Neurology* 47:S86-90.
- Niebroj-Dobosz I, Dziewulska D, Kwiecinski H (2004) Oxidative damage to proteins in the spinal cord in amyotrophic lateral sclerosis (ALS). *Folia Neuropathol* 42:151-156.
- Prudencio M, Hart PJ, Borchelt DR, Andersen PM (2009) Variation in aggregation propensities among ALS-associated variants of SOD1: correlation to human disease. *Hum Mol Genet* 18:3217-3226.
- Rakhit R, Robertson J, Vande Velde C, Horne P, Ruth DM, Griffin J, Cleveland DW, Cashman NR, Chakrabartty A (2007) An immunological epitope selective for pathological monomer-misfolded SOD1 in ALS. *Nat Med* 13:754-759.
- Ralph GS, Radcliffe PA, Day DM, Carthy JM, Leroux MA, Lee DC, Wong LF, Bilsland LG, Greensmith L, Kingsman SM, Mitrophanous KA, Mazarakis ND, Azzouz M (2005) Silencing mutant SOD1 using RNAi protects against neurodegeneration and extends survival in an ALS model. *Nat Med* 11:429-433.
- Renton AE et al. (2011) A hexanucleotide repeat expansion in C9ORF72 is the cause of chromosome 9p21-linked ALS-FTD. *Neuron* 72:257-268.
- Rhoads TW, Lopez NI, Zollinger DR, Morre JT, Arbogast BL, Maier CS, DeNoyer L, Beckman JS (2011) Measuring copper and zinc superoxide dismutase from spinal cord tissue using electrospray mass spectrometry. *Anal Biochem* 415:52-58.
- Rhoads TW, Williams JR, Lopez NI, Morre JT, Bradford CS, Beckman JS (2013) Using theoretical protein isotopic distributions to parse small-mass-difference post-translational modifications via mass spectrometry. *J Am Soc Mass Spectrom* 24:115-124.
- Roberts BR, Tainer JA, Getzoff ED, Malencik DA, Anderson SR, Bomben VC, Meyers KR, Karplus PA, Beckman JS (2007) Structural characterization of zinc-deficient human superoxide dismutase and implications for ALS. *J Mol Biol* 373:877-890.
- Rosen DR, Siddique T, Patterson D, Figlewicz DA, Sapp P, Hentati A, Donaldson D, Goto J, O'Regan JP, Deng HX, et al. (1993) Mutations in Cu/Zn superoxide dismutase gene are associated with familial amyotrophic lateral sclerosis. *Nature* 362:59-62.

- Rumfeldt JA, Lepock JR, Meiering EM (2009) Unfolding and folding kinetics of amyotrophic lateral sclerosis-associated mutant Cu,Zn superoxide dismutases. *J Mol Biol* 385:278-298.
- Sahawneh MA, Ricart KC, Roberts BR, Bomben VC, Basso M, Ye Y, Sahawneh J, Franco MC, Beckman JS, Estevez AG (2010) Cu,Zn-superoxide dismutase increases toxicity of mutant and zinc-deficient superoxide dismutase by enhancing protein stability. *J Biol Chem* 285:33885-33897.
- Son M, Puttapparthi K, Kawamata H, Rajendran B, Boyer PJ, Manfredi G, Elliott JL (2007) Overexpression of CCS in G93A-SOD1 mice leads to accelerated neurological deficits with severe mitochondrial pathology. *Proc Natl Acad Sci U S A* 104:6072-6077.
- Soon CP et al. (2011) Diacetylbis(N(4)-methylthiosemicarbazonato) copper(II) (CuII(at-sm)) protects against peroxynitrite-induced nitrosative damage and prolongs survival in amyotrophic lateral sclerosis mouse model. *J Biol Chem* 286:44035-44044.
- Sreedharan J, Blair IP, Tripathi VB, Hu X, Vance C, Rogelj B, Ackerley S, Durnall JC, Williams KL, Buratti E, Baralle F, de Belleruche J, Mitchell JD, Leigh PN, Al-Chalabi A, Miller CC, Nicholson G, Shaw CE (2008) TDP-43 mutations in familial and sporadic amyotrophic lateral sclerosis. *Science* 319:1668-1672.
- Subramaniam JR, Lyons WE, Liu J, Bartnikas TB, Rothstein J, Price DL, Cleveland DW, Gitlin JD, Wong PC (2002) Mutant SOD1 causes motor neuron disease independent of copper chaperone-mediated copper loading. *Nat Neurosci* 5:301-307.
- Tiwari A, Liba A, Sohn SH, Seetharaman SV, Bilsel O, Matthews CR, Hart PJ, Valentine JS, Hayward LJ (2009) Metal deficiency increases aberrant hydrophobicity of mutant superoxide dismutases that cause amyotrophic lateral sclerosis. *J Biol Chem* 284:27746-27758.
- Tokuda E, Okawa E, Watanabe S, Ono S, Marklund SL (2013) Dysregulation of intracellular copper homeostasis is common to transgenic mice expressing human mutant superoxide dismutase-1s regardless of their copper-binding abilities. *Neurobiol Dis* 54:308-319.
- Tokuda E, Ono S, Ishige K, Watanabe S, Okawa E, Ito Y, Suzuki T (2008) Ammonium tetrathiomolybdate delays onset, prolongs survival, and slows progression of disease in a mouse model for amyotrophic lateral sclerosis. *Exp Neurol* 213:122-128.
- Urushitani M, Ezzi SA, Julien JP (2007) Therapeutic effects of immunization with mutant superoxide dismutase in mice models of amyotrophic lateral sclerosis. *Proc Natl Acad Sci U S A* 104:2495-2500.
- Valentine JS, Pantoliano MW, McDonnell PJ, Burger AR, Lippard SJ (1979) pH-dependent migration of copper(II) to the vacant zinc-binding site of zinc-free bovine erythrocyte superoxide dismutase. *Proc Natl Acad Sci U S A* 76:4245-4249.
- Wang J, Slunt H, Gonzales V, Fromholt D, Coonfield M, Copeland NG, Jenkins NA, Borchelt DR (2003) Copper-binding-site-null SOD1 causes ALS in transgenic mice: aggregates of non-native SOD1 delineate a common feature. *Hum Mol Genet* 12:2753-2764.
- Wang Q, Johnson JL, Agar NY, Agar JN (2008) Protein aggregation and protein instability govern familial amyotrophic lateral sclerosis patient survival. *PLoS Biol* 6:e170.
- Wong PC, Pardo CA, Borchelt DR, Lee MK, Copeland NG, Jenkins NA, Sisodia SS, Cleveland DW, Price DL (1995) An adverse property of a familial ALS-linked SOD1 mutation causes motor neuron disease characterized by vacuolar degeneration of mitochondria. *Neuron* 14:1105-1116.
- Zetterstrom P, Stewart HG, Bergemalm D, Jonsson PA, Graffmo KS, Andersen PM, Brannstrom T, Oliveberg M, Marklund SL (2007) Soluble misfolded subfractions of mutant superoxide dismutase-1s are enriched in spinal cords throughout life in murine ALS models. *Proc Natl Acad Sci U S A* 104:14157-14162.

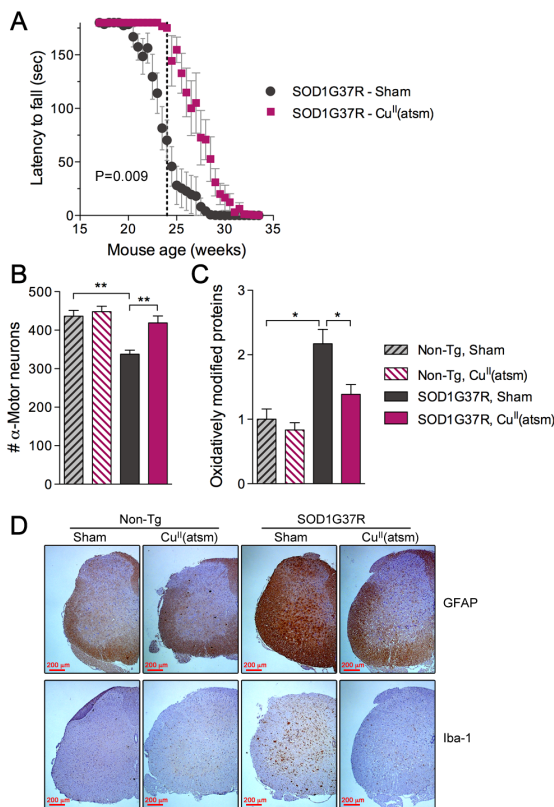


Figure 1. Effects of $\text{Cu}^{\text{II}}(\text{at5m})$ on locomotor function and survival of SOD1G37R mice. (A) Locomotor function of SOD1G37R mice measured as latency to fall on rotarod assay (n=10 sham treated SOD1G37R mice, n=6 $\text{Cu}^{\text{II}}(\text{at5m})$ treated SOD1G37R mice). Dashed line at 24 weeks represents an additional cohort of mice that was culled for all analyses shown in B-D and in Figures 2-5. P value shown represents statistical significance of treatment effect (two-way repeat measures ANOVA). (B) Number of motor neurons present in lumbar region of spinal cords from SOD1G37R mice and non-transgenic littermates. (C) Abundance of oxidatively modified proteins determined using the Oxyblot assay in spinal cord tissue expressed relative to levels detected in sham treated non-transgenic, littermate controls. (D) Representative histology images for GFAP (top row) and Iba-1 (bottom row) immunoreactivity in spinal cord transverse sections. Asterisks in B and C represent statistical significance of data as indicated (* $P < 0.05$, ** $P < 0.01$). n=4-8 for all treatment groups for data in B-D. Error bars represent standard error of the mean.

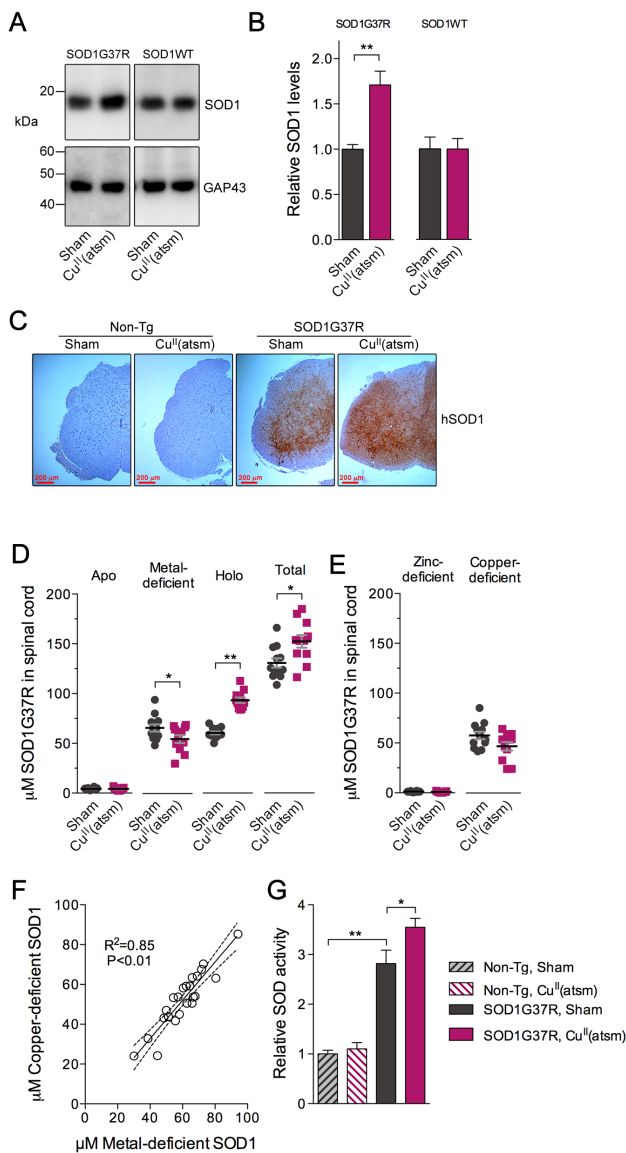


Figure 2. Effects of Cu^{II}(at5m) on SOD1G37R in spinal cord tissue of SOD1G37R mice. (A) Representative western blot images showing effects of Cu^{II}(at5m) on levels of SOD1G37R in spinal cords of SOD1G37R mice and levels of endogenous wild-type SOD1 (SOD1WT) in non-transgenic littermates. Levels of GAP43 are shown as a loading control. (B) Densitometry analysis of western blot analyses represented in (A). (C) Representative histology images for human SOD1 immunoreactivity in spinal cord transverse sections from SOD1G37R mice and non-transgenic littermates. (D) Mutant SOD1 in spinal cords of SOD1G37R mice determined by mass spectrometry showing concentration of apo, metal-deficient, and holo forms of the protein as well as total concentration of the protein. (E) Concentration of zinc-deficient and copper-deficient forms of the metal deficient pool of mutant SOD1. Note same scale on y-axes in D and E. (F) Correlation between levels of metal-deficient SOD1 (from D) and copper-deficient SOD1 (from E) in the spinal cords of sham and Cu^{II}(at5m) treated SOD1G37R mice. There was no correlation between metal-deficient SOD1 and zinc-deficient SOD1 (R²=0.003, P=0.8, data not shown). (G) Activity of SOD in spinal cord samples expressed relative to sham treated non-transgenic, littermate controls. Asterisks indicate statistical significance relative to sham treated SOD1G37R mice or as otherwise indicated (*P<0.05, **P<0.01). n=5-8 for all treatment groups in A, B and G. n=10-11 in D-F. n=4 in C. Error bars represent standard error of the mean.

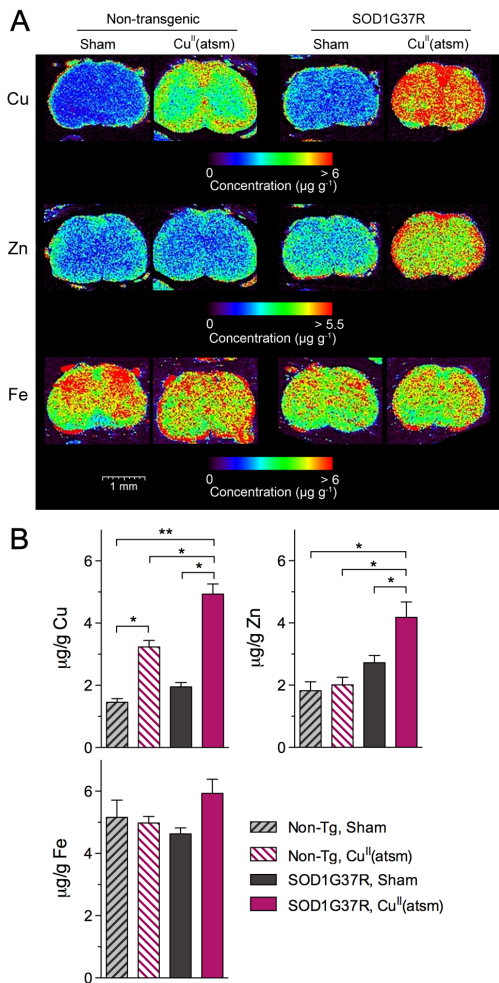


Figure 3. Metal content of spinal cord tissue from SOD1G37R mice and non-transgenic littermates. (A) Representative reconstructed images of LA-ICPMS data showing amounts of Cu, Zn and Fe in spinal cord transverse sections. Pixel color represents metal ion abundance as indicated by spectra shown for each metal ion. (B) Mean data collected from LA-ICPMS analyses as represented in A. Mean data are for whole spinal cord transverse section and therefore include apparent regionalized differences in signal intensity. Asterisks indicate statistical significance as indicated (* $P < 0.05$, ** $P < 0.01$). $n = 4$ for all treatment groups. Error bars represent standard error of the mean.

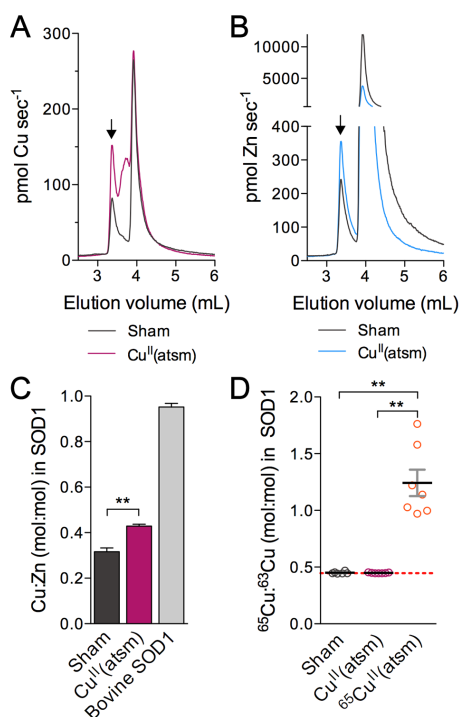


Figure 4. Effects of $\text{Cu}^{\text{II}}(\text{atSm})$ on the metal content of SOD1 in spinal cords of SOD1G37R mice. (A) Mean LC-ICPMS traces showing effects of $\text{Cu}^{\text{II}}(\text{atSm})$ on Cu content of SOD1 in spinal cords of SOD1G37R mice. (B) Mean LC-ICPMS traces showing effects of $\text{Cu}^{\text{II}}(\text{atSm})$ on Zn content of SOD1 in spinal cords of SOD1G37R mice. SOD1 eluted at 3.4 mL as indicated by vertical arrow in A and B. (C) Mean data derived from SOD1 peak in A and B showing effects of $\text{Cu}^{\text{II}}(\text{atSm})$ on the molar ratio of Cu:Zn in SOD1 from spinal cords of SOD1G37R mice. The Cu:Zn ratio in purified bovine SOD1 is shown as a control. (D) Molar ratio of $^{65}\text{Cu}:^{63}\text{Cu}$ in SOD1 from spinal cords of sham, $\text{Cu}^{\text{II}}(\text{atSm})$ and $^{65}\text{Cu}^{\text{II}}(\text{atSm})$ treated SOD1G37R mice determined by LC-ICPMS as per A and B. Horizontal red dashed line shows natural isotopic distribution of $^{65}\text{Cu}:^{63}\text{Cu}$ in biological material (0.45:1). Values above this line indicate an increase in the relative amount of ^{65}Cu in the SOD1. Asterisks indicate statistical significance as indicated (** $P < 0.01$). $n = 6-7$ for all treatment groups except for bovine SOD1 standard in C where $n = 4$. Symbols in D represent data for individual mice. Error bars represent standard error of the mean.

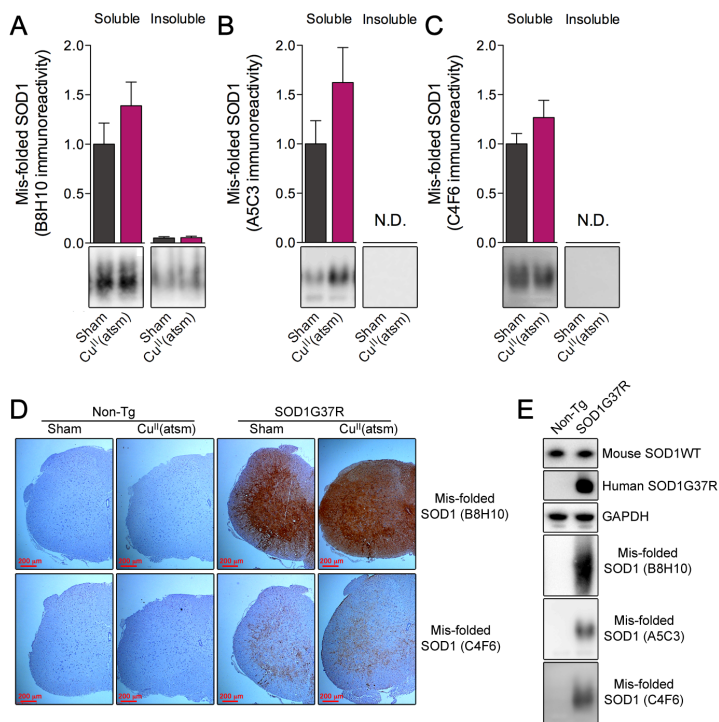


Figure 5. Mis-folded SOD1 in spinal cords of SOD1G37R mice. Levels of mis-folded mutant SOD1 in PBS-soluble and -insoluble fractions of SOD1G37R mouse spinal cords detected using native PAGE and the B8H10 (A), A5C3 (B) and C4F6 (C) antibodies. Values are derived from densitometry analysis of western images (representative images shown) and are expressed relative to immunoreactivity detected in the soluble fraction of sham treated mice. “N.D.” represents non-detectable levels in the insoluble fraction using these antibodies. (D) Representative histology images for mis-folded SOD1 immunoreactivity in spinal cord transverse sections using the B8H10 antibody (top row) and the C4F6 antibody (bottom row). Immunoreactivity using the A5C3 antibody was not detected by histology (not shown). Immunoreactivity for the three antibodies was not detected in non-transgenic mice (E) indicating specificity for the human mutant form of the protein. n=4-5 for all treatment groups and error bars in A, B and C represent standard error of the mean.

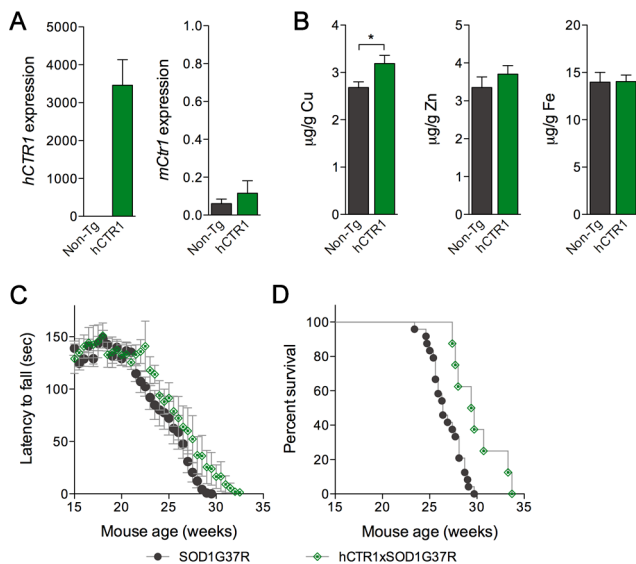


Figure 6. Effects of expressed human copper transporter 1 (*hCTR1*) on locomotor function and survival of SOD1G37R mice. (A) Levels of mRNA for *hCTR1* and *mCtr1* in spinal cords of *hCTR1* mice and non-transgenic littermates (non-Tg). *hCTR1* levels are expressed relative to levels of the endogenous *mCtr1*, and levels of *mCtr1* are expressed relative to levels of endogenous *mActb*. (B) Copper, zinc and iron content of spinal cord tissue from mice expressing *hCTR1* compared to non-transgenic littermates as determined using LA-ICPMS as per Figure 3. $n=6$ for both genotypes in (A) and (B). (C) Locomotor function of SOD1G37R and *hCTR1*xSOD1G37R mice measured as latency to fall on rotarod assay ($n=14$ SOD1G37R mice, $n=8$ *hCTR1*xSOD1G37R mice). (D) Fraction of SOD1G37R and *hCTR1*xSOD1G37R mice alive relative to age ($n=24$ SOD1G37R mice, $n=8$ *hCTR1*xSOD1G37R mice). Regardless of genotype, mice were culled when complete paralysis was present in at least one hind limb and were unable to right themselves within 15 sec after being laid down on their side. Asterisks indicate statistical significance as indicated ($*P<0.05$). Error bars represent standard error of the mean.

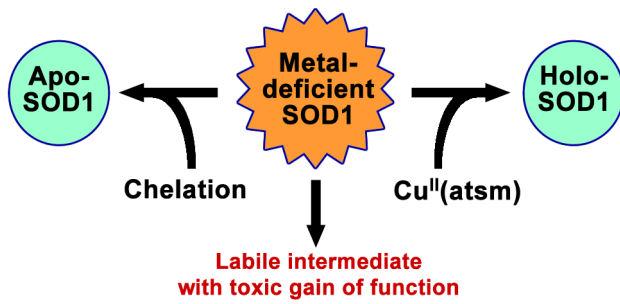


Figure 7. Schematic to indicate how chelation and supplementation therapeutic strategies can both attenuate SOD1 toxicity. Metal-free (apo) and metal-replete (holo) SOD1 are non-toxic; apo-SOD1 is rapidly turned over whereas holo-SOD1 is the stable, functional antioxidant form. Toxicity of the labile, metal-deficient intermediate can be prevented by chelating agents that convert metal-deficient SOD1 to apo-SOD1, or by agents such as Cu^{II}(atism) which convert metal-deficient SOD1 to holo-SOD1.